Drosophila as a Model for Epilepsy: *bss* Is a Gain-of-Function Mutation in the Para Sodium Channel Gene That Leads to Seizures

Louise Parker,*,1 Miguel Padilla,* Yuzhe Du,† Ke Dong† and Mark A. Tanouye*,‡

*Department of Environmental Science, Policy and Management, University of California, Berkeley, California 94720, ‡Department of Molecular and Cell Biology, University of California, Berkeley, California 94720 and †Department of Entomology, Michigan State University, East Lansing, Michigan 48824

ABSTRACT

We report the identification of *bang senseless* (*bss*), a *Drosophila melanogaster* mutant exhibiting seizure-like behaviors, as an allele of the *paralytic* (*para*) voltage-gated Na^+ (Na_V) channel gene. Mutants are more prone to seizure episodes than normal flies because of a lowered seizure threshold. The *bss* phenotypes are due to a missense mutation in a segment previously implicated in inactivation, termed the "paddle motif" of the Na_V fourth homology domain. Heterologous expression of cDNAs containing the *bss¹* lesion, followed by electrophysiology, shows that mutant channels display altered voltage dependence of inactivation compared to wild type. The phenotypes of *bss* are the most severe of the bang-sensitive mutants in Drosophila and can be ameliorated, but not suppressed, by treatment with anti-epileptic drugs. As such, *bss*-associated seizures resemble those of pharmacologically resistant epilepsies caused by mutation of the human Na_V SCN1A, such as severe myoclonic epilepsy in infants or intractable childhood epilepsy with generalized tonic-clonic seizures.

Human epilepsies are a pervasive class of neurological seizure disorder that pose a significant health concern due to the large number of affected individuals, potentially devastating ramifications of untreated seizure episodes, and limitations in anti-epileptic drug options. Especially troublesome are the intractable epilepsies: ~15 million epilepsy sufferers around the world do not respond to currently available medications. While corrective surgery is sometimes a possibility, it can have highly undesirable side effects (SPENCER and HUH 2008). Surprisingly, little is understood about differences that might be responsible for causing intractable epilepsy compared to more benign seizure disorders, and there are few promising new treatments.

A Drosophila model for seizure disorders has been presented on the basis of a collection of 34 neurological mutants that affect seizure susceptibility, including seizure-sensitive and seizure-suppressor mutants (SONG and TANOUYE 2008). This study evaluates the mutant *bang senseless* (*bss¹*) as an intractable epilepsy extension to the model. The *bss¹* mutant is extremely sensitive to seizures, manifesting seizure-like behaviors and paralysis following mechanical, electrical, or visual stimulation. Seizure-like electrical activity is evoked electrophysiologically with a low threshold. We show here that the *bss¹* molecular lesion

affects the *paralytic* (*para*) voltage-gated Na^+ channel (Na_V), the biophysical consequence of which is to alter voltage dependence of channel inactivation. Thus, the *bss¹* lesion also provides a link between fly and human epilepsies that are Na_V channelopathies, a collection of epilepsies gaining in importance as a frequent cause of human disorders (MULLEY *et al.* 2005; LOSSIN 2009).

MATERIALS AND METHODS

Fly stocks: The *bss¹* mutation is an EMS-induced allele of *bang senseless* once thought to be an allele of *bas* (*bang sensitive*) and designated *bas^MW1* (JAN and JAN 1978). Allelic relationships were clarified by GANETZKY and WU (1982) with *bas^MW1* renamed *bss^MW1*; its current designation is *bss¹*. A second allele, *bss²*, is an EMS-induced mutation also known as *bss^PC75* (GANETZKY and WU 1982). The *eas* gene is located at map position 1-53.5 and encodes an ethanolamine kinase (PAVLIDIS *et al.* 1994). The Canton-S strain was used as a wild-type control, unless indicated. Transgenic *UAS-Na_V1-1* and *UAS-Na_V1-1^L1699F* lines were generated by BestGene (Chino Hills, CA). *UAS-paraRNAi* lines were obtained from the Vienna Drosophila RNAi Center. All other lines, including Gal4 driver, P[EP] insertions, and duplication and deletion lines were obtained from the Bloomington Drosophila Stock Center.

Behavior and electrophysiology: Behavioral testing for bang-sensitive (BS) paralysis was performed as described previously (KUEBLER and TANOUYE 2000). Flies were collected <1 day post eclosion and tested for BS paralysis and recovery time 24 hr after collection to mitigate variability due to age. Pools of flies are combined (in total, $n = \sim 100$ for each genotype). For genotypes that display only partial penetrance of BS paralysis, only those flies that displayed paralysis were used for recovery time analysis. *In vivo* recording of seizure-

---

Supporting information is available online at http://www.genetics.org/cgi/content/full/genetics.110.123299/DC1.

[1]*Corresponding author:* Department of Environmental Science, Policy and Management, 135 Life Sciences Addition, University of California, Berkeley, CA 94720. E-mail: louiseparker@berkeley.edu

like activity and seizure threshold determination in adult flies was performed as described previously (KUEBLER and TANOUYE 2000). Flies 2–3 days post eclosion were mounted in wax on a glass slide, leaving the dorsal head, thorax, and abdomen exposed. Stimulating, recording, and ground metal electrodes were made of uninsulated tungsten. Seizure-like activity was evoked by high-frequency electrical brain stimulation (0.5-msec pulses at 200 Hz for 300 msec) and monitored by dorsal longitudinal muscle (DLM) recording. During the course of each experiment, the giant fiber (GF) circuit was monitored continuously as a proxy for holobrain function. For each genotype tested, $n > 20$.

Electrophysiology of heterologously expressed *para* Na$^+$ channels was as described previously (TAN *et al.* 2002; OLSON *et al.* 2008). A DmNa$_v$1-1^{L1699F} cDNA subcloned into the pGH19 expression vector was linearized with *Not*I and transcribed with T7 polymerase (mMESSAGE mMACHINE kit, Ambion). cRNA (1 ng) was co-injected with *tipE* cRNA (1 ng), which encodes a unique transmembrane protein known to be required for robust Na$^+$ channel expression (WARMKE *et al.* 1997). Oocytes obtained surgically from female *Xenopus laevis* were incubated with collagenase (type IA, 1 mg/ml; Sigma) in Ca^{++}-free ND96 medium (96 mM NaCl, 2 mM KCl, 1 mM MgCl$_2$, 5 mM HEPES at pH 7.5). Oocytes were then incubated in normal ND96 medium containing 1.8 mM CaCl$_2$, 5 mM pyruvate, 0.5 mM theophylline, and 50 mg/ml gentamicin, and Na$^+$ currents were recorded by a two-microelectrode voltage clamp. Borosilicate glass electrodes were filled with filtered 3 M KCl in 0.5% agarose and had resistance <1.0 MΩ. Currents were measured using an oocyte clamp (OC725C, Warner Instruments), Digidata interface (1200A, Axon Instruments), and pCLAMP9 software (Axon Instruments). All experiments were performed at room temperature (20°–22°). Capacitative transients and linear leak current were corrected by P/N subtraction or subtraction in tetrodotoxin (20 nM).

The voltage dependence of sodium channel conductance (*G*) was calculated by measuring the peak current at test potentials ranging from −80 to +65 mV in 5-mV increments and divided by ($V - V_{rev}$), where *V* is the test potential and V_{rev} is the reversal potential for sodium ion. Peak conductance values were normalized to the maximum peak conductance (G_{max}) and fitted with a two-state Boltzmann equation of the form $G/G_{max} = [1 + \exp(V - V_{1/2})/k]^{-1}$, in which *V* is the potential of the voltage pulse, $V_{1/2}$ is the voltage for half-maximal activation, and *k* is the slope factor.

The voltage dependence of sodium channel fast inactivation was determined by using 100-msec inactivating prepulses ranging from −120 to 25 mV in 5-mV increments from a holding potential of −120 mV, followed by test pulses to −10 mV for 20 msec. The peak current amplitude during the test depolarization was normalized to the maximum current amplitude and plotted as a function of the prepulse potential. Data were fitted with a two-state Boltzmann equation of the form $I/I_{max} = [1 + \exp(V - V_{1/2})/k]^{-1}$, in which *I* is the peak sodium current, I_{max} is the maximal current evoked, *V* is the potential of the voltage prepulse, $V_{1/2}$ is the half-maximal voltage for inactivation, and *k* is the slope factor.

To determine the steady-state slow inactivation, oocytes were held at prepulse potentials ranging from −100 to −10 mV in 10-mV increments for 60 sec. A 100-msec recovery pulse to −120 mV and a 20-msec test pulse to −10 mV were given before returning to the holding potential of −120 mV. The peak current amplitude during the test depolarization was normalized to the maximum current amplitude and plotted as a function of the prepulse potential. The data were fitted with a two-state Boltzmann equation of the form $I/I_{max} = [1 + \exp(V - V_{1/2})/k]^{-1}$, in which I_{max} is the maximal current evoked, *V* is the potential of the voltage pulse, $V_{1/2}$ is

the half-maximal voltage for inactivation, and *k* is the slope factor.

To determine recovery from fast inactivation, sodium channels were inactivated by a 100-msec depolarizing pulse to −10 mV and then repolarized to −120 mV for an interval of variable durations followed by a 20-msec test pulse to −10 mV. The peak current during the test pulse was divided by the peak current during the inactivating pulse and plotted as a function of duration time between the two pulses.

Recovery from slow inactivation was measured using a 60-sec depolarization to −10 mV followed by variable intervals at −120 mV and a subsequent 10-msec test pulse to −10 mV. The available current recorded with the test pulse was normalized to peak current recorded immediately prior to the recovery protocol.

Molecular biology: The Na$_V$1-1 adult isoform of *para* encodes a functional Na$^+$ channel when expressed heterologously in Xenopus channels (WARMKE *et al.* 1997). The L1699F missense mutation was introduced into pGH19-Na$_V$1-1 (corresponding to Na$_V$1-1 L1676F, a C → T point change at 5026 bp) using primers L1699F-F (CCATCTTAGGTCTTGTATTTAGCGATATTATCGAGAAGTACTTCG) and L1699F-R (CGAAGTACTTCTCGATAATATCGCTAAATACAAGACCTAAGATGG) with the Quikchange XL II kit (Stratagene). The entire Na$_V$1-1^{L1699F} sequence was determined to confirm the point change and ensure that no additional PCR-induced mutations were introduced. Na$_V$1-1 and Na$_V$1-1^{L1699F} cDNAs were excised from the pGH19 vector using *Kpn*I and *Nhe*I and then subcloned into pUAST cut with *Kpn*I and *Xba*I.

Data analysis: Chi-square tests were used to compare the penetrance of seizures. Student's *t*-test and ANOVA were used to compare recovery times and seizure thresholds across genotypes, as appropriate. For ANOVA analysis, where the null hypothesis was rejected by the overall F ratio, multiple comparisons of data sets were performed by Fisher's least significant difference with *t*-test significance set at $P < 0.05$. For Figures 2, 4 and 5, error bars represent standard error of the mean, and statistical significance is indicated by *$P < 0.05$, **$P < 0.01$, and ***$P < 0.0001$.

RESULTS

bss¹ **behavior—seizure sensitivity and tonic-clonic-like activity:** The behavior of *bss¹* mutants is similar to other mutants of the BS paralytic class such as *eas^{PC80}*, *sda$^{iso7.8}$*, and *tko^{25t}* mutants (ROYDEN *et al.* 1987; PAVLIDIS *et al.* 1994; ZHANG *et al.* 2002). Under normal conditions, *bss¹* flies display unexceptional feeding, grooming, and mating behaviors and show wild-type phototaxis and geotaxis responses. Overall activity levels are unaltered, and flies are neither sluggish nor hyperactive. Abnormal behavior is induced in *bss¹* mutants by mechanical shock (a "bang"). The resulting behavioral phenotype is complex (Figure 1A) with six distinguishable phases: seizure; initial paralysis; tonic-clonic-like activity; recovery seizure; refractory recovery during which behaviorally normal flies cannot be induced to have further seizures; and, finally, complete recovery.

The initial seizure for *bss¹* is similar to other BS mutants, lasting several seconds and characterized by leg shaking, abdominal muscle contractions, wing flapping and scissoring, and proboscis extensions. Initial paralysis is also typical of BS mutants: *bss¹* flies are immobile and
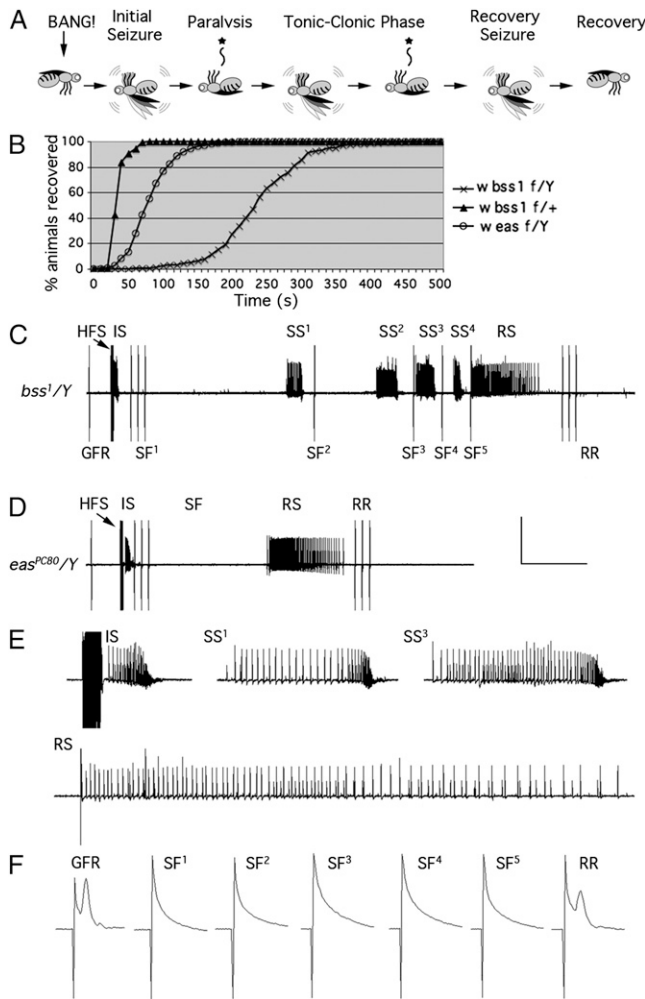
FIGURE 1.—Drosophila *bss¹* mutant behavior and electrophysiology seizure-like phenotypes. (A) Cartoon depicting stereotypic behavioral phenotype of *bss¹* flies subjected to a mechanical shock (10-sec vortex: BANG): initial seizure-like behavior, followed by complete paralysis and then a tonic-clonic-like period that is unique to *bss¹* and not evident in other BS mutant genotypes. One clonus-like event is depicted, but the number can vary, as can the duration of the period. The tonic-clonic-like period is followed by a recovery seizure, and the fly then recovers. Not depicted is a quiescent period of variable duration often observed between the recovery seizure and recovery, as well as the refractory period during which flies are resistant to further seizures that occurs immediately following recovery. (B) For *bss¹/Y* hemizygous males, recovery time from behavioral paralysis is substantially longer than for *bss¹/+* heterozygous females or for another BS mutant, *eas^PC80/Y*. (C) Electrical recording from a DLM fiber showing seizure-like neuronal activity and synaptic failure in a *bss¹/Y* animal subjected to a 4-V high-frequency electrical stimulus (HFS), as well as single-pulse stimuli to trigger the GF circuit, allowing assessment of synaptic function (giant fiber response, GFR). Following an initial seizure (IS) is a period of synaptic failure within which GF stimulation fails to evoke a DLM response (SF^1–5), unlike that seen prior to the seizure. As depicted, during the period of synaptic failure, spontaneous secondary seizures are observed (SS^1–4). Although in this trace four secondary seizures are observed, the number is variable. A final recovery seizure (RS) is observed, and shortly thereafter, GF system transmission is restored (response recovery, RR). Vertical calibration bar: 40 mV

unresponsive to mechanical stimulus, as described previously (GANETZKY and WU 1982). Unlike other BS mutants, initial paralysis in *bss¹* homozygotes is followed by an extended period of tonic-clonic-like activity (Figure 1A). During this period, the fly is mainly quiescent, resembling a tonic phase. The quiescence is broken up by multiple bouts of clonus-like activity. As in other BS mutant flies, *bss¹* shows a recovery seizure, then a refractory period, followed by complete recovery. *bss¹* recovery time is longer than for other BS mutants; mean recovery time for *bss¹* is ~240 sec, compared with *sda* or *eas* at 38 and 81 sec, respectively (Figure 1B and Figure 2B). Interestingly, analysis of the larval neuromuscular junction in *bss¹* animals indicates that motoneurons are hyperexcitable, displaying an abnormal long-term facilitation after repeated stimulation resulting in multiple action potentials and a large, prolonged excitatory junction potential (EJP), where, in contrast, wild-type animals show only a single-action potential and a single small EJP (JAN and JAN, 1978; GANETZKY and WU 1982).

The *bss¹* allele is a severely seizure-sensitive mutation and a strong semidominant that causes the most extreme phenotype of the BS mutants. In comparison, *eas* and *tko* mutants behave as recessives, while *sda* mutants are weakly semidominant. BS seizure-like behaviors and paralysis were observed in heterozygous *bss¹/+* flies at high penetrance (95%), similar to previous reports (GANETZKY and WU 1982). Behavioral phenotypes seen in *bss¹* homozygotes and heterozygotes are generally similar, the main difference being that heterozygotes lack tonic-clonic-like activity, thereby more closely resembling *eas* or *sda* homozygous mutants in behavior. There is also a large reduction in recovery time from ~240 sec in the homozygote to ~50 sec in the heterozygote (Figure 1B and Figure 2B). Behavioral phenotypes of heterozygotes are sensitive to genetic background. For example, although ordinarily highly penetrant, there can be considerable variation in the percentage of paralyzed heterozygous flies (50–95%), depending on the genetic background. Genetic background can also influence recovery time, as discussed below.

Extreme seizure sensitivity in *bss¹* and the electrophysiology of tonic-clonic-like spontaneous firing: The electrophysiology phenotype of *bss¹* is generally similar to that seen in other BS mutants, although more extreme in some aspects. As was the case for behavior, electrophysiology is normally unexceptional in *bss¹*

in all panels. Horizontal calibration bar: 10 sec in (C) and (D), 1.5 sec in (E), and 10 msec in (F). (D) For *eas^PC80/Y*, HFS stimulation causes an initial seizure, synaptic failure, and a recovery seizure; however, no secondary seizures are observed. (E) At a higher sweep speed, depicted are initial seizure, secondary seizures, and recovery seizure from the recording in B. (F) At a higher sweep speed, depicted are GF response (GFR), synaptic failures (SF), and response recovery (RR) from the recording in B.

mutants as determined by using the adult giant fiber system neural circuit as proxy (TANOUYE and WYMAN 1980). Thus, for example, single-pulse stimulation of the giant fiber produced evoked muscle potential responses in the dorsal longitudinal muscles that were normal in appearance and had a threshold of 2.04 ± 0.48 V and a latency of 2.07 msec. Also normal was the ability to follow high-frequency stimulation and respond to short interpulse twin-pulse intervals.

Seizure-like electrical activity in *bss¹* mutants can be evoked with high-frequency stimuli (HFS; 0.5-msec stimuli at 200 Hz for 300 msec) at exceptionally low stimulation voltages (PAVLIDIS and TANOUYE 1995; KUEBLER and TANOUYE 2000; LEE and WU 2002). Seizure-like activity following HFS consisted of aberrant high-frequency firing (>100 Hz) lasting for ∼1 sec, which was present in the dorsal longitudinal muscle and all other muscle fibers and motoneurons examined (Figure 1, C and E). This *bss¹* seizure-like phenotype is qualitatively similar to that seen for other BS genotypes and normal flies, differing only in the HFS voltage required for eliciting it (*i.e.*, the seizure threshold), but otherwise indistinguishable in subsequent electrical activity (Figure 1D). For *bss¹* males, the seizure threshold is 4.4 V HFS. This is substantially lower than for wild-type males (30.1 V HFS) and slightly lower than for *eas* and *sda* BS mutant males (5.13 and 6.2 V HFS, respectively). Thus, using the criterion of HFS threshold, *bss¹* mutants are about seven times more seizure-sensitive than wild-type flies.

After an initial seizure, the next aspect of the electrophysiology phenotype for *bss¹* mutants is the sudden failure of the giant fiber system neural circuit to drive muscle potentials in the dorsal longitudinal muscle. This is termed a "synaptic failure" period as it has been shown to be due to transmission failure at many central synapses (Figure 1F; PAVLIDIS and TANOUYE 1995); it is likely the cause of behavioral paralysis in *bss¹* mutants and in other BS genotypes. However, whereas the period of synaptic failure is short in most BS mutants, for example, ∼38 sec in *sda*, for *bss¹*, it is longer and more complex, apparently reflecting the complexity observed behaviorally as tonic-clonic-like activity (Figure 1, A and C).

For the purpose of describing the electrophysiology of the *bss¹* tonic-clonic-like period, it is convenient to consider three seizure types: (1) initial seizure, occurring immediately after HFS; (2) secondary seizures, occurring within the tonic-clonic-like interval; and (3) recovery seizure, occurring immediately prior to long-term recovery of the giant fiber system neural-circuit response (Figure 1, C and E). Initial and secondary seizures resemble each other in waveform and duration; recovery seizures are somewhat different in waveform and longer in duration, although the significance of this is unclear. In young *bss¹* flies (1 day post eclosion), the tonic-clonic-like period is fairly short, ∼45 sec, and contains only one secondary seizure. In older *bss¹* flies

(7 days old), the tonic-clonic-like period is longer, ∼75 sec, and typically contains three to four secondary seizures, although up to eight have been observed. This is consistent with observations of longer behavioral recovery times in older *bss¹* flies.

Continuous stimulation of the giant fiber system neural circuit during the tonic-clonic-like period shows that, during the tonic intervals, there is no transmission through the circuit to the dorsal longitudinal muscle fiber (Figure 1F). From this, we infer that the lack of transmission is likely due to synaptic failure at many central synapses as proposed for BS paralysis (PAVLIDIS and TANOUYE 1995). Interestingly, approximately coincident with each secondary seizure, transmission through the giant fiber system neural circuit is transiently restored. That is, if a single-pulse stimulation is delivered to the giant fiber system within the period of the secondary-seizure burst, the stimulation is capable of evoking a muscle potential in the dorsal longitudinal muscle. Surprisingly, if a single-pulse stimulation is delivered to the giant fiber system anywhere outside of a secondary seizure burst (*i.e.*, within the apparent tonic interval), it is ineffective at evoking a muscle potential (compare Figure 1, C and F). From these observations, we propose that tonic-clonic-like periods following initial seizure arise from periods of synaptic failure responsible for tonic intervals and a restoration of transmission at central synapses that are requisite for the bouts of clonus-like activity. What remains unclear is why secondary seizures lead to synaptic failure, while the recovery seizure does not. Following the recovery seizure, synaptic transmission not only is retained, but also is refractory to failure. Moreover, secondary seizures occur only in *bss¹* mutants; only initial and recovery seizures are observed in *sda* and *eas* mutants (Figure 1D).

Similar to behavior, the tonic-clonic-like period observed electrophysiologically for *bss¹* is sensitive to genetic background. For example, secondary seizures are completely absent in *bss¹*/+ heterozygotes. In these flies, initial seizure and synaptic failure are followed by a recovery seizure, without any occurrence of secondary seizures. Electrophysiological recordings from these heterozygotes resemble those taken from *sda* and *eas* flies, although with increased seizure thresholds (19.1 HFS V for *bss¹*/+ flies; Figure 5E).

A missense mutation of the *para Na_V* gene is responsible for *bss¹*: Genetic localization by duplication/deletion mapping is somewhat problematic for *bss¹* because the semidominant nature of its phenotype makes it difficult to distinguish homozygotes from heterozygotes. Since *bss¹*/+ heterozygote recovery time is shorter than homozygote recovery time, this feature of the phenotype can be used for mapping. However, since recovery time can also vary substantially with age, genetic background, and other factors, all comparisons were between age-matched 2-day-old siblings arising from the same cross to minimize variations due to these sources. Initial de-

termination of the *bss¹* chromosomal location indicated the 14E-15A9 cytological interval of the X chromosome (Figure 2, A–C). In particular, localization for *bss¹* is based on its inclusion in the *Dp(1)r+75c* duplication, which reduces recovery time in *bss¹/Y* hemizygotes (Figure 2B) (15A9: position of its proximal breakpoint), and its exclusion from the *Df(1)19 f* deletion, which has no effect on recovery time in *bss¹/Df(1)19 f* heterozygotes, in comparison to *bss¹/Df(1)r-D1* heterozygotes, which show increased recovery time (Figure 2C) (14E: approximate position of its proximal breakpoint). This is consistent with the combined findings from other overlapping chromosomal aneuploids of the region (Figure 2, A–C).

Initial mapping of *bss¹* suggested a location farther to the right on the X chromosome than had been previously indicated (GANETZKY and WU 1982). This, coupled with uncertainties of deficiency/duplication mapping due to *bss¹* semidominance, prompted us to generate a more definitive location by recombination mapping with subsequent molecular determination of crossover sites (fine-structure recombinational mapping) (Figure 2D, Table S1). Recombination events were defined between *bss¹* and one of two molecularly defined transposon insertions (P[EP]s). We scored 8977 male progeny from females of the genotype $w^- \, bss¹ \, f^-/w^-$ *P[EP]EY00852*. Four animals were found in which a crossover event occurred between *bss¹* and *P[EP]*. The position of *P[EP]EY00852* at 16,342,911 bp results in a derived position for *bss¹* of 0.04 cM (or ∼10 kb) to the right of this location (Figure 2D). Similarly, we examined 2903 male progeny from females of the genotype $w^- \, bss¹ \, f^-/w^-$ *P[EP]EY08038* and found nine animals in which a crossover event occurred between *bss¹* and *P[EP]*. The location of this insertion at 16,427,296 bp gives a derived position for *bss¹* at 0.34 cM (or ∼75 kb) to the left of this location (Figure 2D). These data are consistent with our deficiency/duplication mapping that placed *bss¹* in the 14E-15A9 cytological region that corresponds to ∼16,400,000–16,700,000 bp.

Fine-structure recombinational mapping was used to determine more precisely the location of *bss¹*. This mapping took advantage of the fact that in the chromosomal region containing *P[EP]EY00852* there are 40 DNA sequence polymorphisms that can be used to molecularly distinguish the $w^- \, bss¹ \, f^-$ parental chromosome from the *P[EP]EY00852* parental chromosome (Table S1). Each of the four male progeny with a crossover between *bss¹* and *P[EP]* is expected to display one of the parental patterns up until the site of the crossover event and, at that point, abruptly shift to the other parental pattern. Each of the crossover locations was determined (Table S1) for the four recombinant chromosomes; these locations were ∼4, 8, 8, and 11 kb to the right of the insertion, respectively. The fourth recombination event, which provides the most useful information because it lies the farthest to the right of *P[EP]*, took place between a TTG 3-bp deletion at
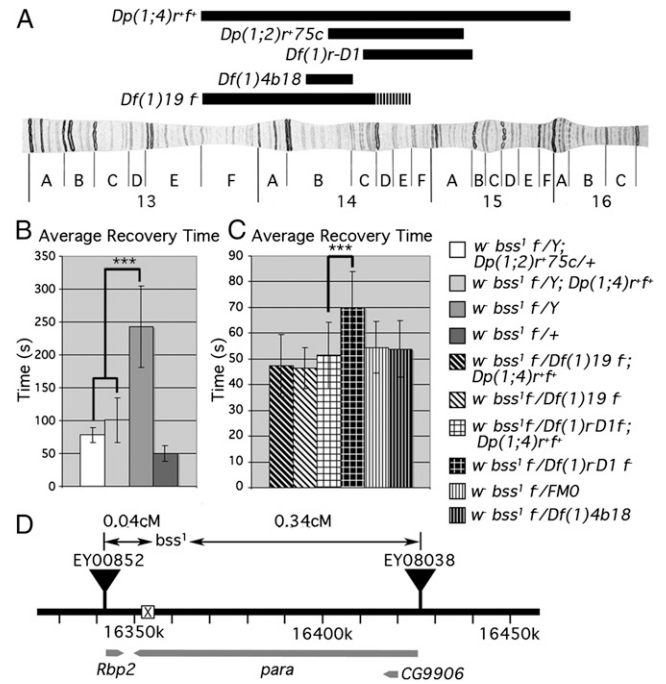

FIGURE 2.—*bss¹* maps to within the *para* gene. (A) Cytological region affected by chromosomal duplications and deletions used in mapping. Hatched region in *Df(1)19* indicates inconsistency between cytological and molecular breakpoints. (B and C) Mean recovery time for *bss¹* flies in the presence of duplications or deletions. Error bars represent standard error of the mean; significance was determined by Student's *t*-test. (B) The *Dp(1;2)r+75c* (14B13-15A9) includes *bss¹*, providing one boundary at 15A9. This is indicated by the finding that *bss¹/Y;Dp* flies have a significantly shorter mean recovery time than sibling control *bss¹/Y* flies (78 ± 3 sec, $n = 137$, *vs.* 243 ± 6 sec, $n = 109$, $P = 1.6 \times 10^{-73}$). Confirmatory findings are observed with the larger *Dp(1;4)r+f+* = 13F–16A7 (103 ± 5 sec, $n = 100$ test, *vs.* 232 ± 6 sec, $n = 105$ control, $P = 4.4 \times 10^{-37}$). (C) *Df(1)19* (13F–14E) fails to include *bss¹*, providing a boundary at 14E. This is indicated by the finding that the mean recovery time of *bss¹/Df* flies (46 ± 0.8 sec, $n = 113$) is not significantly longer than sibling control *bss¹/Df;Dp(1;4)r+f+* flies (47 ± 1.1 sec, $n = 134$, $P = 0.52$). Similar findings are observed with the smaller *Df(1)4b18* (14B8–14C1) (54 ± 1.0 sec, $n = 98$ test; 54 ± 1.0 sec, $n = 105$ control; $P = 0.65$). These results are in contrast to those observed using the larger *Df(1)r-D1* (14C5–15B1) (70 ± 1.3 sec, $n = 109$ test; *vs.* 51 ± 1.2 sec, $n = 122$ control; $P = 1.3 \times 10^{-20}$) that must contain *bss¹*. We conclude that the *bss* gene lies within the 14E-15A9 region and that the presence of a wild-type copy in a hemizygote mutant fly can reduce the duration of the behavioral phenotype to resemble that of a heterozygote (B), while the absence of a wild-type copy in a *bss¹* heterozygote can increase mean recovery time (C). Statistical significance key here, and in Figures 4 and 5, is *$P < 0.05$, **$P < 0.01$, or ***$P < 0.0001$. (D) Recombination mapping placed *bss¹* between *P[EP]* element insertions *EY00852* and *EY08038*. Sequencing of recombinant chromosomes to track 40 polymorphisms detected between parental chromosomes placed *bss¹* to the right of a 3-bp deletion at residue 16353592 (marked with an X) and indicates that the *bss¹* lesion is in *para*. See File S1 and Table S1 for more detail.

location 16,353,592 and a A → G point change at location 16,354,339. This 747-bp segment lies within the extensive *para* 3′ UTR (SONG and TANOUYE 2007),

3.5 kb downstream of the *para* stop codon. Since the *bss¹* lesion must lie farther to the right of the crossover point, it is either within the remaining *para* 3′ UTR or, more likely, within the C-terminal coding sequence of *para*.

The fine-structure mapping definitively rules out the possibility that *bss¹* is a lesion in *Rbp2*, since all recombination events occurred to the right of the gene. It also makes it unlikely that *bss¹* is a lesion in *CG9906* because all recombination events occurred much farther to the left of this gene; however, we cannot rule out this possibility. We therefore sought to determine the molecular lesion responsible for the *bss¹* mutation by sequencing all 31 *para* exons, including intron/exon boundaries, as well as the single *CG9906* exon. In comparison to the published genome sequence (ADAMS *et al.* 2000), in *bss¹* we found a single nucleotide change in *para* exon 30, a C → T point change in the coding sequence that lies at position 16,360,824. This change causes an amino acid substitution from leucine to phenylalanine, corresponding to L1699 in the ParaPA sequence (GenBank accession NP_523371; Figure 3A). The position of this point change in exon 30, 17.9 kb to the right of P[EP]00852, is entirely consistent with the recombination mapping data for *bss¹*. Only two other nucleotide changes were found in *para* and both were silent polymorphisms, one in exon 30 and another in exon 31; no changes were found in *CG9906*. Thus, L1699F is the only amino acid sequence change in the *bss¹ para* gene, the only candidate for the *bss¹* lesion. The *bss¹* lesion was confirmed by sequencing exon 30 from Canton-S, Oregon R, and *w¹¹¹⁸* strains that all showed the wild-type sequence (Figure 3A). The wild-type strains also carried the same silent polymorphisms found in *bss¹*, suggesting that they may be sequencing errors in the published sequence. A second mutation, *bss²*, has been reported as being of independent origin (GANETZKY and WU 1982). Consistent with this, examination of the *bss²* sequence shows multiple polymorphisms in the *para* 3′ UTR compared to the *bss¹* sequence. Surprisingly, however, and identical to *bss¹*, L1699 in *bss²* is substituted by a phenylalanine residue also as the result of a C5364T point change. The L1699 location corresponds to a highly conserved residue in the third membrane-spanning segment (S3b) of homology domain IV of the Na$_V$ channel (Figure 3, B and C).

Phenotypic severity of *para^bss1* can be manipulated by altering expression levels—Reduced expression suppresses phenotypes: Since *bss¹* and *bss²* mutations are alleles of *para*, we rename them here *para^bss1* and *para^bss2*, respectively. The finding that they are allelic to *para* is surprising, given that none of the many other *para* mutations previously identified demonstrate bang sensitivity. In fact, all other *para* mutations examined for seizure susceptibility are loss-of-function alleles that have been shown to cause seizure resistance with thresholds above that of wild-type flies. Also, they have all been shown to act as seizure-suppressor mutations, capable of
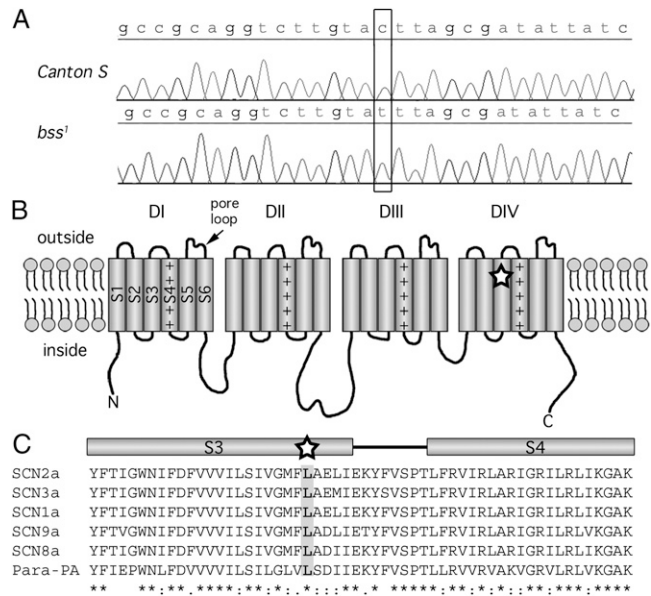

FIGURE 3.—The *bss¹* lesion causes an L → F change in a highly conserved residue of Para. (A) Sequencing of *para* exons from *bss¹* mutants identified a C → T point change at nucleotide 5364 in the paraRA cDNA, which is not present in Canton S, Oregon R, or *w¹¹¹⁸* strains, resulting in a L1699F residue change. (B) Cartoon depicting the structure of Na$_V$ channels. The L1699 residue lies within homology domain IV, transmembrane segment S3 (star) of the Para protein. (C) L1699 is highly conserved across mammalian neuronal Na$_V$ channels.

reducing seizure severity in other BS mutants (KUEBLER *et al.* 2001; SONG and TANOUYE 2007). This implies that *para^bss1* is a gain-of-function mutation of *para*, consistent with its dominant phenotype.

Further evidence for the gain-of-function nature of the *para^bss1* allele is revealed by altering expression levels: reducing *para^bss1* expression substantially suppressed BS phenotypes. Reduction of *para^bss1* expression by para RNA interference utilized the Gal4-UAS system. In hemizygous *para^bss1* males, when Na$_V$ expression in all neurons was reduced using *Elav-Gal4^3A* to drive *UAS-paraRNAi*, only 65% of flies showed BS paralysis, a reduction of 35% compared to sibling controls that showed 100% BS paralysis (test: *para^bss1/Y; Elav-Gal4^3A/ UAS-paraRNAi ×2*; control: *para^bss1/Y; Elav-Gal4^3A/+*) (Figure 4A). In contrast, heterozygous *para^bss1/+* females showed nearly complete suppression: only 1.6% of flies are BS compared to 87% of sibling controls (genotype of test: *para^bss1/para⁺; Elav-Gal4^3A/UAS-paraRNAi ×2*; genotype of sibling control: *para^bss1/para⁺; Elav-Gal4^3A/+*). This finding suggests that the total amount of *para^bss1* gene product is important in determining the severity of the phenotype and fits with the observation that *para^bss1* hemizygote and heterozygote phenotypes differ significantly in severity. However, unexpected expression asymmetries due to differential *paraRNAi* knockdown or wild-type/mutant competition for membrane sites are also possibilities.

Some insight into interpreting the *paraRNAi* results may be found from examining effects in wild-type animals. Interestingly, utilizing a stronger neuronal Gal4 driver (*Elav-Gal4^C155*) resulted in complete lethality; that is, no flies were observed of the test genotype compared to 196 control siblings (test: *Elav-Gal4^C155*; *UAS-paraRNAi x2*; control: *Elav-Gal4^C155/+; TM6b/+*). A similar level of lethality is seen in a *para^bss1/+* heterozygote background. We interpret the lethality as an extreme *para* loss of function.

Consistent with this interpretation, a weaker pan-neuronal Gal4 driver (*1407-Gal4*) produced a temperature-sensitive paralytic phenotype, similar to that displayed by weaker *para* loss-of-function mutants (Suzuki *et al.* 1971; Siddiqi and Benzer 1976; Wu and Ganetzky 1980). Flies (112/121) were reversibly paralyzed when tested at 38°, compared to 0/120 sibling controls (test: *1407-Gal4/+; UAS-paraRNAi x2/+*; control: *1407-Gal4/+; TM6b/+*). These observations indicate that *paraRNAi* was effective at reducing *para* expression, thereby phenocopying *para* hypomorphic and null alleles, although with the necessity of using different Gal4 drivers.

Expression of *para* can also be altered by manipulating levels of TipE, an enhancer of *para* loss-of-function mutations (Ganetzky 1986; Jackson *et al.* 1986; Feng *et al.* 1995; Warmke *et al.* 1997; Hodges *et al.* 2002). The mechanism for this interaction is not completely clear; however, it appears to differ from *paraRNAi*. In contrast to the enhancement of *para* loss-of-function phenotypes, in *para^bss1/+; tipE^1/+* flies, penetrance of BS phenotypes was significantly reduced compared to controls, and in *para^bss1/+; tipE^1/tipE^1* flies, penetrance was reduced even further (Figure 4B). However, we saw no suppression of BS phenotypes in *para^bss1/Y* hemizygotes (126/126 *para^bss1/Y; tipE^1/tipE^1* flies tested were BS).

Phenotypic severity of *para^bss1* can be manipulated by altering expression levels—Increased expression enhances phenotypes: If *para^bss1* is a gain-of-function mutation, we reasoned that increasing the amount of mutant protein should increase the severity of the BS phenotype. We were able to show this by manipulating endogenous *para^bss1* expression levels utilizing the GAL4/UAS system. The pan-neuronal *Elav-Gal4^C155* driver was used to activate the UAS sequence in the *P[EP]EY08038* insertion that lies immediately upstream of the *para* gene (*e.g.*, in *cis* orientation with respect to the mutant gene). Test animals were generated where the *P[EP]* is *cis* to *para^bss1*, thereby driving overexpression of the mutated gene (genotype: *w para^bss1 P[EP]EY08038/Elav-Gal4^C155 para^+*) (Figure 4C). The test flies have a much longer recovery time compared to sibling controls (genotype: *w para^bss1 P[EP]EY08038/para^+*) that lack the *Elav-Gal4^C155* driver (116 *vs.* 67 sec; Figure 4E). These data indicate that, by increasing the levels of Para^bss1 mutant protein through overexpression, we can significantly increase the severity of the BS phenotype, thereby providing strong
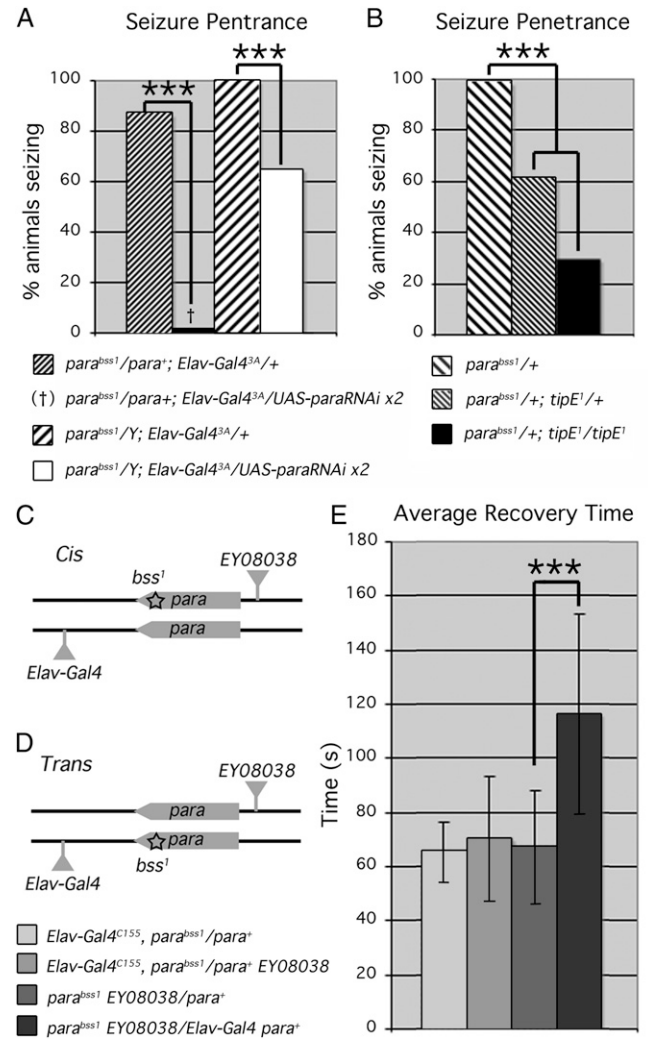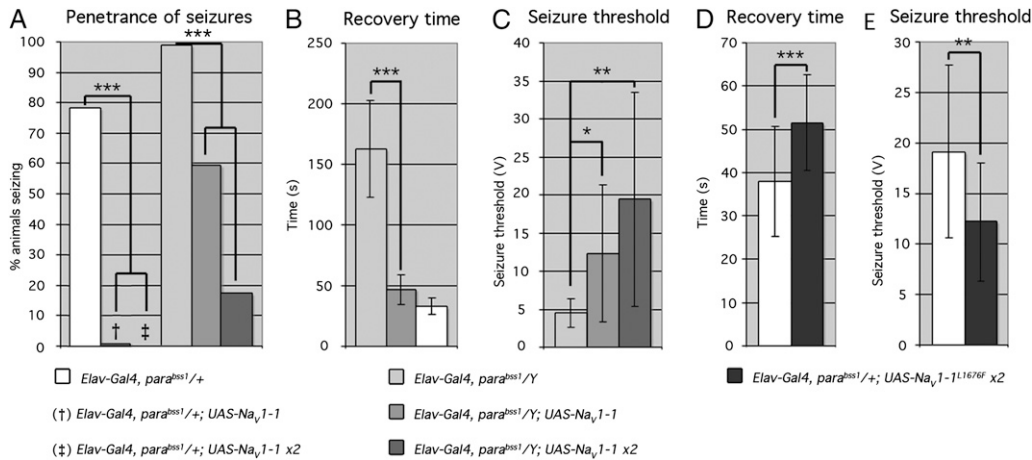

Figure 4.—Genetic manipulation of endogenous *para^bss1* expression or function alters seizure phenotypes. (A and B) Penetrance of seizures is decreased when *para* expression or function is suppressed. (A) Decreasing *para* expression by driving *UAS-paraRNAi* pan-neuronally using *Elav-Gal4* suppresses seizure occurrence both in *para^bss1/+* heterozygous females (1.6% of flies are BS compared to 87% of sibling controls; $P = 3.4 \times 10^{-24}$) and in *para^bss1/Y* hemizygous males (65% of flies are BS compared to 100% of sibling controls; $P = 2.7 \times 10^{-4}$). (B) Reduced TipE levels in *para^bss1/+* heterozygote females suppress bang sensitivity. *para^bss1/+; tipE^1/+* animals are 60.9% BS while *para^bss1/+; tipE^1/tipE^1* animals are 29.6% BS; control siblings are 99% BS, and $P = 8.9 \times 10^{-25}$. (C–E) Ectopic expression of endogenous *para^bss1* exacerbates seizure phenotypes. Pan-neuronal ectopic expression of *para* in a *bss1* background was achieved using (C) *cis* and (D) *trans* configurations of the *bss1* mutation relative to *P[EP]* insertion EY08038. (E) When the *bss1* lesion is in *trans* to the *P[EP]* insertion, mean recovery time is virtually unchanged compared to control siblings (test: *Elav-Gal4^C155*, *bss1/para+ EY08038* = 70 ± 1.9 sec, $n = 148$, vs. control: *Elav-Gal4^C155*, *bss1/para+* = 65 ± 1.2 sec, $n = 84$; $P > 0.05$) whereas when *bss1* is in *cis* to the P[EP] insertion, mean recovery time is significantly increased (test: *bss1 EY08038/Elav-Gal4^C155 para^+* = 116 ± 3.5 sec, $n = 119$, vs. control: *bss1 EY08038/para^+* 67 ± 2 sec, $n = 118$; $P = 1.03 \times 10^{-25}$), indicating that increased levels of mutant Para^bss1 protein result in more severe seizure phenotypes. All error bars represent standard error of the mean. Statistical significance was calculated for A and B by chi-square test and for E by Student's *t*-test.

FIGURE 5.—Ectopic expression of *para* isoform Na$_V$1-1 wild-type and mutant forms alters seizure severity. (A–C) Pan-neuronal expression of Na$_V$1-1, driven by *Elav-Gal4* with one or two copies of *UAS-Na$_V$1-1*, in a *para^{bss1}* background suppresses seizure phenotypes in comparison to sibling controls. (A) Penetrance of bang sensitivity in *para^{bss1}/+* heterozygotes is drastically reduced from 78% ($n = 166$) to 0.8% ($n = 252$) with one copy of *UAS-Na$_V$1-1*, while two copies completely suppresses the phenotype ($n = 125$) $P = 6.7 \times 10^{-64}$. Bang sensitivity of *para^{bss1}/Y* hemizygotes is reduced from 98.9% ($n = 88$) to 59.6% ($n = 193$) with one copy and to 17.3% ($n = 104$) with two copies of *UAS-Na$_V$1-1*, $P = 6.4 \times 10^{-16}$. (B) Mean recovery time of *para^{bss1}/Y* hemizygotes is reduced from 163 ± 4.6 sec ($n = 78$) to 47 ± 1.6 sec ($n = 59$) with one copy of *UAS-Na$_V$1-1*, $P = 8.4 \times 10^{-42}$ and shows a similar recovery time to *para^{bss1}/+* heterozygotes (33 ± 0.8 sec, $n = 77$). (C) Average seizure threshold of *para^{bss1}/Y* hemizygotes is significantly increased from 4.5 ± 0.3 V ($n = 37$) to 12.3 ± 2.6 V ($n = 12$) with one copy and to 19.4 ± 3.2 V ($n = 14$) with two copies of *UAS-Na$_V$1-1*; $P = 1.6 \times 10^{-8}$. (D and E) Pan-neuronal expression of Na$_V$1-1^{L1699F}, driven by *Elav-Gal4* with two copies of *UAS-Na$_V$1-1^{L1699F}* in a *para^{bss1}* background, enhances seizure phenotypes. (D) Mean recovery time of *para^{bss1}/+* heterozygotes increases from 38 ± 1 sec, $n = 113$, in sibling controls to 52 ± 1 sec, $n = 146$, with two copies of *UAS-Na$_V$1-1^{L1699F}*; $P = 1.3 \times 10^{-17}$. (E) Average seizure threshold decreases from 19.1 ± 1.8 V ($n = 24$) in sibling controls to 12.2 ± 1.3 V ($n = 18$) with two copies of *UAS-Na$_V$1-1^{L1699F}*; $P = 3.8 \times 10^{-3}$. In all cases, error bars represent standard error. Statistical significance was calculated for A by chi-square test; for B, D, and E by Student's *t*-test; and for C by ANOVA.

phenotypic support that a gain-of-function lesion in *para* is responsible for bang sensitivity.

We also generated animals where the *P[EP]* is *trans* to *para^{bss1}*, that is, in *cis* with respect to the wild-type *para* gene and thereby driving expression of the wild type, not the mutant, form of *para* (genotype: *Elav-Gal4^{C155} para^{bss1}/w para$^+$ P[EP]EY08038*) (Figure 4D). These flies have a similar recovery time compared to sibling controls (genotype: *Elav-Gal4^{C155} para^{bss1}/w para$^+$*) that lack *P[EP]* (70 *vs.* 65 sec; Figure 4E). These data indicate that increasing the level of endogenous Para$^+$ protein through overexpression does not seem to improve the BS recovery time phenotype above that of the heterozygote. A similar finding was observed in the duplication/deficiency analysis where a duplication of the *para* region in a heterozygous *para^{bss1}/+* animal has no effect on recovery time (Figure 2C) and is seemingly a consequence of the gain-of-function nature of *para^{bss1}* and its complicated gene-dosage relationships.

Expression of wild-type and *para^{L1699F}* mutant transgenes: A wild-type *para$^+$* transgene was constructed and found to be effective at suppressing *para^{bss1}* phenotypes. Constructs utilized the cDNA of the Na$_V$1-1 *para* isoform, the most common splice variant in adults (OLSON *et al.* 2008; LIN *et al.* 2009), expressed in all neurons with an *Elav-Gal4^{c155}* driver. Bang-sensitive paralysis was completely suppressed (0% BS) in *para^{bss1}/+* heterozygotes carrying two copies of the transgene; in comparison, sibling controls showed 78.3% BS (Figure 5A) (test genotype: *Elav-Gal4^{C155} para^{bss1}/+; UAS-Na$_V$1-1 x2*; control genotype: *Elav-Gal4^{C155} para^{bss1}/+*). The wild-type trans-

gene was also effective in rescuing phenotypes in hemizygous *para^{bss1}/Y* flies; bang sensitivity was suppressed to 17.3% (control: 100% BS; Figure 5A) (test genotype: *Elav-Gal4^{C155} para^{bss1}/Y; UAS-Na$_V$1-1 x2*; control genotype: *Elav-Gal4^{C155} para^{bss1}/Y*). Electrophysiologically, for these flies the seizure threshold increases to 19.4 V in animals carrying the transgene, compared to the lower 4.8-V seizure threshold of sibling control flies (Figure 5C).

The most straightforward explanation for rescue of BS phenotypes by wild-type Na$_V$1-1 is that the cDNA is biologically active *in vivo* and rescues in a manner similar to genetic duplications carrying the *para$^+$* genomic region. We expect, however, that the explanation likely is more complex since control crosses indicate that, although the cDNA transgene is effective at rescuing the gain-of-function phenotypes of *para^{bss1}*, it is ineffective at rescuing the loss-of-function phenotypes in *para^{ts1}*, *para^{ST76}*, and *para^{lk2}* mutants. These differences may be related to the complexity of the *para* gene that produces a large number of different splice variants; 53 different variants have been characterized to date, and the cDNA Na$_V$1-1 used here corresponds to only one of these variants (O'DOWD *et al.* 1995; OLSON *et al.* 2008; LIN *et al.* 2009). It is unlikely that a single isoform could effectively rescue the entire range of *para* functions.

A mutant *para* transgene was constructed by engineering the L1699F mutation into the Na$_V$1-1 cDNA. The expectation was that since the *para^{bss1}* allele is a gain-of-function mutation, the Na$_V$1-1^{L1699F} transgene would confer BS phenotypes on wild-type flies. The results obtained showed the mutant transgene to be less

effective than expected: only a few flies carrying it displayed bang-sensitive paralysis (1.6%, 4/250 BS flies), although the average recovery period for the few flies paralyzed (33 sec) resembled the recovery period of *para^bss1^/+* heterozygotes (genotype of test flies: *Elav-Gal4^C155^/+; UAS-Na_V_1-1^L1699F^/UAS-Na_V_1-1^L1699F^*). Increasing copy numbers of either UAS or Gal4 transgenes in an attempt to increase penetrance resulted in larval lethality. *Nrv2-Gal4*, another pan-neuronal driver, showed a similarly low penetrance of BS.

We then questioned whether or not the causative *para^bss1^* lesion was indeed the L1699F residue change. If not, then the *Na_V_1-1^L1699F^* transgene should behave as a wild-type transgene and rescue *para^bss1^* phenotypes. The results obtained showed that the mutant transgene could not rescue *para^bss1^*, but instead exacerbated BS phenotypes. *para^bss1^/+* heterozygous females carrying the transgene were tested for recovery time and electrophysiological seizure threshold compared to their control siblings (test: *Elav-Gal4^C155^, para^bss1^/+; UAS-Na_V_1-1^L1699F^ x2/+*; control: *Elav-Gal4, para^bss1^/+*). A significant increase in recovery time was observed from 38 to 49 sec (Figure 5D), as well as a decrease in seizure threshold from 19.1 to 12.1 V (Figure 5E) in test flies carrying the transgene compared to their control siblings. From this, we conclude that *Na_V_1-1^L1699F^* does not behave as a wild-type transgene; rather, the results are most consistent with L1699F being responsible for the *para^bss1^* lesion with low phenotypic penetrance of the mutant transgene.

Na_V_1-1^L1699F^ channels show altered inactivation: The functional consequences of the L1699F mutation in cDNA Na_v_1-1 were examined by expressing wild-type and mutant channels in Xenopus oocytes followed by electrophysiological testing. Mutant channel expression in oocytes appears to be substantially reduced compared to wild-type channel controls (~10-fold) as indicated by significantly decreased peak current amplitudes (Figure 6A). Mutant and wild-type channels are similar in their voltage dependence and kinetics of channel activation (Figure 6, B and G). In contrast, inactivation for the mutant channel was significantly different from that of wild type. Voltage dependence of fast inactivation is shifted to more positive potentials for mutant channels, relative to wild type ($V_{1/2} = -38.3 \pm 1.63$ mV compared to -49.43 ± 2.48 mV, $P < 0.01$; Figure 6, C and G). While voltage dependence of slow inactivation was not altered, the slope factor (k) was significantly changed in the mutant channel ($k = 5.32 \pm 0.5$ compared to 9.26 ± 1.85 for wild type, $P < 0.01$; Figure 6, D and G). Recovery from fast or slow inactivation was comparable in mutant and wild-type channels (Figure 6, E and F). Although a heterologous expression assay cannot be said to definitively account for the effect of the L1699F lesion *in vivo*, it indicates that a likely consequence of this mutation is the alteration of fast inactivation such that neurons expressing Para^bss1^ will be more excitable, giving rise to increased risk of seizure.

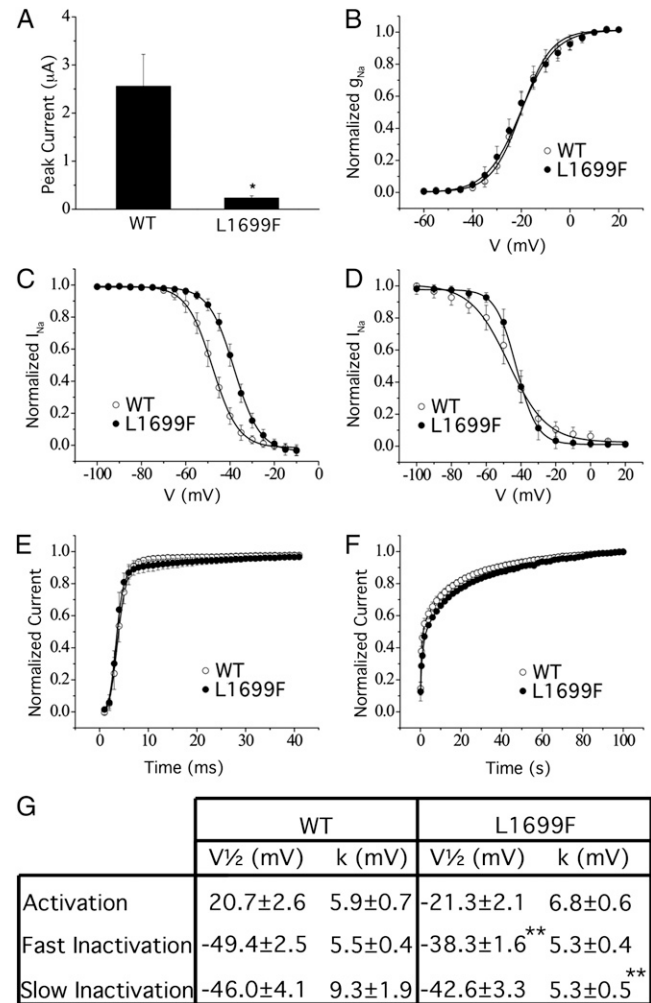| G	WT		L1699F	
	V½ (mV)	k (mV)	V½ (mV)	k (mV)
Activation	20.7±2.6	5.9±0.7	-21.3±2.1	6.8±0.6
Fast Inactivation	-49.4±2.5	5.5±0.4	-38.3±1.6**	5.3±0.4
Slow Inactivation	-46.0±4.1	9.3±1.9	-42.6±3.3	5.3±0.5**

FIGURE 6.—Channel inactivation is altered by the L1699F mutation. (A) Histogram comparing amplitudes of peak current from Na_V_1-1 wild-type (WT) and Na_V_1-1^L1699F^ mutant channels. Peak current was elicited by a 20-msec depolarization to -10 mV from the holding potential of -120 mV. The same amount of cRNA (5 ng/oocyte) of wild-type or mutant channels was injected into oocytes, and a recording was made at day 4. (B) Voltage dependence of activation in wild-type and mutant channels is comparable. (C) Voltage dependence of fast inactivation in mutant channels shows a shift to more positive potentials relative to wild-type channels. (D) Voltage dependence of slow inactivation in mutant channels is comparable to wild type; however, the slope value is altered. Recovery from (E) fast inactivation and (F) slow inactivation is comparable in wild-type and mutant channels. (G) Gating properties of Na_V_1-1 and Na_V_1-1^L1699F^ channels. $V_{1/2}$ activation voltages are similar for wild type and mutant; however, the $V_{1/2}$ fast inactivation difference is significant. Although $V_{1/2}$ slow inactivation is comparable for wild-type and mutant channels, the slope value (k) is significantly decreased. For A–F, graphical representations of recording protocols are shown above each graph; for details, see MATERIALS AND METHODS.

DISCUSSION

para is an essential gene, well studied for its basic Na_V_ channel function, but not considered previously as a candidate for *bss*. The gene comprises 31 exons under-

going alternate splicing to generate at least 53 distinct transcripts, with additional variation generated by RNA editing (O'Dowd *et al.* 1995; Reenan *et al.* 2000; Hodges *et al.* 2002; Olson *et al.* 2008; Lin *et al.* 2009). The *para^{bss1}* gain-of-function mutation, with its seizure-sensitive phenotype, is unlike any of the other 68 reported *para* alleles, the best known of which are partial loss-of-function alleles, such as *para^{ts1}* and *para^{ST76}*, which induce temperature-sensitive paralysis due to loss of Na$^+$-based action potentials (Suzuki *et al.* 1971; Siddiqi and Benzer 1976; Wu and Ganetzky 1980). Indeed, *para* loss-of-function mutations are seizure-resistant seizure suppressors. For example, *para^{ST76}* mutants have a seizure threshold of 65 V compared to 30.1 V for wild-type flies, indicative of seizure resistance. It is also one of the most effective seizure suppressors in combination with other BS mutations (Kuebler *et al.* 2001).

Na$_V$ channel α-subunits are composed of four homologous domains (DI–DIV), each containing six transmembrane segments (S1–S6) (Catterall 2000). The ion pore is formed centrally by the collective organization of S5 and S6 segments from each domain; surrounding the ion pore are the four voltage sensors, each of the S1–S4 segments from the different domains. Studies of voltage sensors in K$_V$ and Na$_V$ channels have defined the S3b–S4 helix-turn-helix as a modular unit termed a "paddle motif" (Alabi *et al.* 2007; Bosmans *et al.* 2008; Catterall *et al.* 2008). The paddle moves at the protein–lipid interface, driving activation of the voltage sensors and opening or closing of the pore. The location of the *para^{bss1}* L1699F lesion is in the S3b helix of the DIV paddle. The leucine residue at this position is highly conserved in voltage-gated channels, which were present in SCN1A homologs from all species examined. The leucine residue is also conserved in all neuronal forms of human Na$_V$ channels (Figure 3C) and in several K$_v$ channels, including Kv2.1 (sequence not shown). We show that, in a Na$_V$1-1 cDNA, the functional effect of the L1699F mutation is to shift the voltage of fast inactivation to more positive potentials, with no effect on activation (Figure 6). This conforms to current thinking on Na$_V$ paddle domains: that the voltage sensor paddles of DI–DIII drive channel activation, whereas the DIV paddle drives channel inactivation (Bosmans *et al.* 2008).

Recent molecular genetic advances have led to the concept that the idiopathic epilepsies are a family of channelopathies (Catterall *et al.* 2008; Reid *et al.* 2009). In humans, there are nine different Na$_V$ α-subunits, five of which are neuronally expressed. Excitability in different neuronal cell types is regulated by differential expression of the α-subunits and association with one or more of four ancillary β-subunits (Catterall 2000). Idiopathic epilepsies are attributed to mutations in five α-subunits (SCN1A, -2A, -3A, -8A, -9A) and in one β-subunit (SCN1B) (Spampanato *et al.* 2001; Catterall *et al.* 2008; Reid *et al.* 2009). Initially, epilepsy pathologies were attributed to gain-of-function mutations caus-

ing hyperexcitability via accelerated recovery from channel inactivation (*e.g.*, SCN1A R1648H; Spampanato *et al.* 2001) or a negative shift in the voltage dependence of steady-state inactivation (*e.g.*, SCN1A W1204R; Spampanato *et al.* 2003). Hyperexcitability from persistent Na$^+$ current contributes to depolarization, shaping repetitive firing, generating rhythmicity, and amplification. The more recent discovery that many SCN1A epilepsies are caused by loss-of-function mutations, intuitively expected to cause hypoexcitability, has altered current thinking (Madia *et al.* 2006; Suls *et al.* 2008). SCN1A mutagenesis in the mouse has suggested that loss-of-function mutations may have a greater effect in inhibitory interneurons and a lesser effect in excitatory pyramidal cells (Ogiwara *et al.* 2007; Tang *et al.* 2009). The explanation for this is that SCN1A is more highly expressed in inhibitory interneurons while other Na$_V$ channel subtypes are more highly expressed in pyramidal neurons. Accordingly, loss of SCN1A function results in a loss of inhibition at the level of the neural circuit, causing a net increase in nervous system hyperexcitability.

The link between molecular deficit and clinical phenotype, however, is poorly characterized due to clinical heterogeneity in familial epilepsies that is thought to arise from differences in genetic background (Osaka *et al.* 2007; Mahoney *et al.* 2009). In SCN1A, lesions that result in truncated proteins are almost always associated with the intractable disorders severe myoclonic epilepsy in infants (SMEI) or intractable childhood epilepsy with generalized tonic-clonic seizures (ICEGTC). However, 50% of the SCN1A lesions identified in SMEI or ICEGTC patients are missense mutations, functional studies of which have shown no consistent relationship between alterations in channel properties and clinical phenotype. Neither does there appear to be a correlation between lesion location and clinical presentation, despite large-scale studies identifying hundreds of novel lesions in patients (Depienne *et al.* 2009; Lossin 2009; SCN1a variant database at http://www.molgen.ua.ac.be/SCN1AMutations/Home/Default.cfm). Thus, our understanding of the molecular mechanisms of Na$_V$-linked epilepsies is still very limited. The Drosophila *para^{bss1}* mutation contributes a novel finding to the field in that it is the first Na$_V$ missense mutation to show gain-of-function qualities both *in vivo* and in heterologous expression assays. It demonstrates that both gain-of-function and loss-of-function mutations could contribute to the wide clinical spectrum of epilepsies associated with Na$_V$ channels.

Our study has provided the basis for a Drosophila model of Na$_V$-linked intractable epilepsies, a devastating condition due to its manifestation during infancy. In demonstrating that *para^{bss1}* is a gain-of-function allele, we show that there may be more than one molecular mechanism for inducing seizures, and the location of the *para^{bss1}* lesion suggests that the DIV paddle motif may

be a key region for gain-of-function mutations. Further study of this genetically tractable system will enable us to dissect the relative contributions of causative mutation, modifying genetic factors, and environmental influences in expression of seizure-like phenotypes, as well as to identify potential new treatments.

LITERATURE CITED

Adams, M. D., S. E. Celniker, R. A. Holt, C. A. Evans, J. D. Gocayne *et al.*, 2000 The genome sequence of *Drosophila melanogaster*. Science **287:** 2185–2195.

Alabi, A. A., M. I. Bahamonde, H. J. Jung, J. I. Kim and K. J. Swartz, 2007 Portability of paddle motif function and pharmacology in voltage sensors. Nature **450:** 370–376.

Bosmans, F., M. F. Martin-Eauclair and K. J. Swartz, 2008 Deconstructing voltage sensor function and pharmacology in sodium channels. Nature **456:** 202–209.

Catterall, W. A., 2000 From ionic currents to molecular mechanisms: the structure and function of voltage-gated sodium channels. Neuron **26:** 13–25.

Catterall, W. A., S. Dib-Hajj, M. H. Meisler and D. Pietrobon, 2008 Inherited neuronal ion channelopathies: new windows on complex neurological diseases. J. Neurosci. **28:** 11768–11777.

Depienne, C., O. Trouillard, C. Saint-Martin, I. Gourfinkel-An, D. Bouteiller *et al.*, 2009 Spectrum of SCN1A gene mutations associated with Dravet syndrome: analysis of 333 patients. J. Med. Genet. **46:** 183–191.

Feng, G., P. Deak, M. Chopra and L. M. Hall, 1995 Cloning and functional analysis of TipE, a novel membrane protein that enhances Drosophila Para sodium channel function. Cell **82:** 1001–1011.

Ganetzky, B., 1986 Neurogenetic analysis of Drosophila mutations affecting sodium channels: synergistic effects on viability and nerve conduction in double mutants involving *tip-E*. J. Neurogenet. **3:** 19–31.

Ganetzky, B., and C. F. Wu, 1982 Indirect suppression involving behavioral mutants with altered nerve excitability in *Drosophila melanogaster*. Genetics **100:** 597–614.

Hodges, D. D., D. Lee, C. F. Preston, K. Boswell, L. M. Hall *et al.*, 2002 *tipE* regulates Na$^+$-dependent repetitive firing in Drosophila neurons. Mol. Cell. Neurosci. **19:** 402–416.

Jackson, F. R., S. D. Wilson and L. M. Hall, 1986 The *tip-E* mutation of Drosophila decreases saxitoxin binding and interacts with other mutations affecting nerve membrane excitability. J. Neurogenet. **3:** 1–17.

Jan, Y. N., and L. Y. Jan, 1978 Genetic dissection of short-term and long-term facilitation at the Drosophila neuromuscular junction. Proc. Natl. Acad. Sci. USA **75:** 515–519.

Kuebler, D., and M. A. Tanouye, 2000 Modifications of seizure susceptibility in Drosophila. J. Neurophysiol. **83:** 998–1009.

Kuebler, D., H. G. Zhang, X. Ren and M. A. Tanouye, 2001 Genetic suppression of seizure susceptibility in Drosophila. J. Neurophysiol. **86:** 1211–1225.

Lee, J., and C. -F. Wu, 2002 Electroconvulsive seizure behavior in Drosophila: analysis of the physiological repertoire underlying a stereotyped action pattern in bang-sensitive mutants. J. Neurosci. **22:** 11065–11079.

Lin, W. H., D. E. Wright, N. I. Muraro and R. A. Baines, 2009 Alternative splicing in the voltage-gated sodium channel DmNa$_V$ regulates activation, inactivation, and persistent current. J. Neurophysiol. **102:** 1994–2006.

Lossin, C., 2009 A catalog of SCN1A variants. Brain Dev. **31:** 114–130.

Madia, F., P. Striano, E. Gennaro, M. Malacarne, R. Paravidino *et al.*, 2006 Cryptic chromosome deletions involving SCN1A in severe myoclonic epilepsy of infancy. Neurology **67:** 1230–1235.

Mahoney, K., S. J. Moore, D. Buckley, M. Alam, P. Parfrey *et al.*, 2009 Variable neurologic phenotype in a GEFS+ family with a novel mutation in SCN1A. Seizure **18:** 492–497.

Mulley, J. C., I. E. Scheffer, S. Petrou, L. M. Dibbens, S. F. Berkovic *et al.*, 2005 SCN1A mutations and epilepsy. Hum. Mutat. **25:** 535–542.

O'Dowd, D. K., J. R. Gee and M. A. Smith, 1995 Sodium current density correlates with expression of specific alternatively spliced sodium channel mRNAs in single neurons. J. Neurosci. **15:** 4005–4012.

Ogiwara, I., H. Miyamoto, N. Morita, N. Atapour, E. Mazaki *et al.*, 2007 Na(v)1.1 localizes to axons of parvalbumin-positive inhibitory interneurons: a circuit basis for epileptic seizures in mice carrying an *Scn1a* gene mutation. J. Neurosci. **27:** 5903–5914.

Olson, R. O., Z. Liu, Y. Nomura, W. Song and K. Dong, 2008 Molecular and functional characterization of voltage-gated sodium channel variants from *Drosophila melanogaster*. Insect Biochem. Mol. Biol. **38:** 604–610.

Osaka, H., I. Ogiwara, E. Mazaki, N. Okamura, S. Yamashita *et al.*, 2007 Patients with a sodium channel alpha 1 gene mutation show wide phenotypic variation. Epilepsy Res. **75:** 46–51.

Pavlidis, P., and M. A. Tanouye, 1995 Seizures and failures in the giant fiber pathway of Drosophila bang-sensitive paralytic mutants. J. Neurosci. **15:** 5810–5819.

Pavlidis, P., M. Ramaswami and M. A. Tanouye, 1994 The Drosophila *easily shocked* gene: a mutation in a phospholipid synthetic pathway causes seizure, neuronal failure, and paralysis. Cell **79:** 23–33.

Reenan, R. A., C. J. Hanrahan and B. Ganetzky, 2000 The *mle(napts)* RNA helicase mutation in Drosophila results in a splicing catastrophe of the *para* Na$^+$ channel transcript in a region of RNA editing. Neuron **25:** 139–149.

Reid, C. A., S. F. Berkovic and S. Petrou, 2009 Mechanisms of human inherited epilepsies. Prog. Neurobiol. **87:** 41–57.

Royden, C. S., V. Pirrotta and L. Y. Jan, 1987 The *tko* locus, site of a behavioral mutation in *D. melanogaster*, codes for a protein homologous to prokaryotic ribosomal protein S12. Cell **51:** 165–173.

Siddiqi, O., and S. Benzer, 1976 Neurophysiological defects in temperature-sensitive paralytic mutants of *Drosophila melanogaster*. Proc. Natl. Acad. Sci. USA **73:** 3253–3257.

Song, J., and M. A. Tanouye, 2007 A role for *para* sodium channel gene 3′ UTR in the modification of Drosophila seizure susceptibility. Dev. Neurobiol. **67:** 1944–1956.

Song, J., and M. A. Tanouye, 2008 From bench to drug: human seizure modeling using Drosophila. Prog. Neurobiol. **84:** 182–191.

Spampanato, J., A. Escayg, M. H. Meisler and A. L. Goldin, 2001 Functional effects of two voltage-gated sodium channel mutations that cause generalized epilepsy with febrile seizures plus type 2. J. Neurosci. **21:** 7481–7490.

Spampanato, J., A. Escayg, M. H. Meisler and A. L. Goldin, 2003 Generalized epilepsy with febrile seizures plus type 2 mutation W1204R alters voltage-dependent gating of Na(v)1.1 sodium channels. Neuroscience **116:** 37–48.

Spencer, S., and L. Huh, 2008 Outcomes of epilepsy surgery in adults and children. Lancet Neurol. **7:** 525–537.

Suls, A., K. G. Claeys, D. Goossens, B. Harding, R. Van Luijk *et al.*, 2008 Microdeletions involving the SCN1A gene may be common in SCN1A-mutation-negative SMEI patients. Hum. Mutat. **27:** 914–920.

Suzuki, D., T. Grigliatti and R. Williamson, 1971 Temperature-sensitive mutations in *Drosophila melanogaster*, VII. A mutation (*para*^{ts}) causing reversible adult paralysis. Proc. Natl. Acad. Sci. USA **68:** 890–893.

Tan, J. G., Z. Q. Liu, Y. Nomura, A. L. Goldin and K. Dong, 2002 Alternative splicing of an insect sodium channel gene generates pharmacologically distinct sodium channels. J. Neurosci. **22:** 5300–5309.

Tang, B., K. Dutt, L. Papale, R. Rusconi, A. Shankar *et al.*, 2009 A BAC transgenic mouse model reveals neuron subtype-specific effects of a generalized epilepsy with febrile seizures plus (GEFS+) mutation. Neurobiol. Dis. **35:** 91–102.

Tanouye, M. A., and R. J. Wyman, 1980 Motor outputs of giant nerve fiber in Drosophila. J. Neurophysiol. **44:** 405–421.

WARMKE, J. W., R. A. REENAN, P. WANG, S. QIAN, J. P. ARENA *et al.*, 1997 Functional expression of Drosophila Para sodium channels. Modulation by the membrane protein TipE and toxin pharmacology. J. Gen. Physiol. **110:** 119–133.

WU, C. F., and B. GANETZKY, 1980 Genetic alteration of nerve membrane excitability in temperature-sensitive paralytic mutants of *Drosophila melanogaster*. Nature **286:** 814–816.

ZHANG, H., J. TAN, E. REYNOLDS, D. KUEBLER, S. FAULHABER *et al.*, 2002 The Drosophila *slamdance* gene: a mutation in an aminopeptidase can cause seizure, paralysis and neuronal failure. Genetics **162:** 1283–1299.

Communicating editor: R. ANHOLT

GENETICS

Drosophila as a Model for Epilepsy: *bss* Is a Gain-of-Function Mutation in the Para Sodium Channel Gene That Leads to Seizures

Louise Parker, Miguel Padilla, Yuzhe Du, Ke Dong and Mark A. Tanouye

FILE S1

Recombinational mapping of *bss¹* using P[EP]00852

Verification of the P[EP] line: The P[EP]00852 line was obtained from the Bloomington stock center, is homozygous viable and shows no obvious phenotype. Although the insertion was previously molecularly characterized, we verified its chromosomal location by PCR amplification from *P[EP]00852* genomic DNA using primers Pinv Repeat (5'-CGGGACCACCTTATGTTATTTC-3') and Rbp2 exon1 (5'-GCTAATTGGTGTGGTGACACT-3'), followed by sequencing of the product. Our analysis showed that *P[EP]00852* is indeed inserted into the X chromosome at 16,342,911bp.

Generating recombinant males: *w-, bss¹, f* homozygote females were crossed to *P[EP]00852/Y* hemizygote males. The female F₁ progeny (genotype *w-, bss¹, f /w-, P[EP]00852*) were allowed to mate with their F₁ male siblings (genotype *w- bss¹, f /Y*) and 8977 male F₂ progeny were collected and scored for the presence of the P[EP] insertion (using the mini-*white⁺* gene present in the construct), the presence of *bss¹* (by determining whether they were BS or not) and the presence of the *f* mutation. Recombinants between *bss¹* and *P[EP]00852* were defined as animals that either had both *w⁺* eyes and displayed BS paralysis (*w-, P[EP]EY00852, bss¹, f*), or animals that had w- eyes and showed no BS paralysis (*w-, bss⁺, f⁺*). The presence or absence of the *f-* mutation allowed us to determine the chromosomal order of *bss¹* and *P[EP]00852* relative to *f*.

TABLE S1

Fine structure recombinational mapping places *bss¹* within the *para* gene

	Polymorphism	Molecular position on X chromosome	Parental Chromosomes		Recombinant Chromsomes			
	A	B	C	D	E	F	G	H
			w-, bss¹, f	*w-, P[EP] EY00852*	#1 *w-, bss⁺ f⁺*	#2 *w-, P[EP] EY00852, bss¹, f*	#3 *w-, bss⁺ f⁺*	#4 *w-, bss⁺ f⁺*
Rbp2 3' UTR	G->A	16346125	Y	N	Y	N	Y	Y
	T->A	16346760	N	Y	N	Y	N	N
	G->A	16346769	N	Y	N	Y	N	N
	G->A	16346840	N	Y	N	Y	N	N
	C insertion	16346946	N	Y	N	Y	N	N

TA->GG	16346958	N	Y	N	Y	N	N
A insertion	16347422	Y	N	N	N	Y	Y
A->T	16347492	Y	N	N	N	Y	Y
G->C	16347729	Y	N	N	N	Y	Y
T->C	16347855	Y	N	N	N	Y	Y
T->A	16348287	Y	N	N	N	Y	Y
CG->TT	16349045	Y	N	N	N	Y	Y
C->T	16349993	Y	N	N	N	Y	Y
TATTCGTATTCG insertion	16350041	Y	N	N	N	Y	Y
C->T	16350101	Y	N	N	N	Y	Y
TGTGTGTATATGTGTG deletion	16350165	Y	N	N	N	Y	Y
AT deletion	16350268	Y	N	N	N	Y	Y
C->T	16350296	Y	N	N	N	Y	Y
C->T	16350409	Y	N	N	N	Y	Y
CG insertion	16350431	Y	N	N	N	Y	Y
TT insertion	16350536	N	Y	Y	Y	N	N
A->C	16350747	Y	N	N	N	Y	Y
A->G	16351689	Y	N	N	Y	N	Y
A->C	16351903	Y	N	N	Y	N	Y
TGTGTGTG deletion	16352045	Y	N	N	Y	N	Y
TTTT deletion	16352276	Y	N	N	Y	N	Y
TT insertion	16352374	Y	N	N	Y	N	Y
G->T	16352771	Y	N	N	Y	N	Y
C->T	16353164	Y	N	N	Y	N	Y
TT deletion	16353420	Y	N	N	Y	N	Y
T->A	16353430	Y	N	N	Y	N	Y
TTG deletion	16353574	Y	N	N	Y	N	Y
A->G	16354339	Y	N	N	Y	N	N
T->A	16355033	Y	N	N	Y	N	N
T->A	16355317	Y	N	N	Y	N	N
T->C	16355465	Y	N	N	Y	N	N
T deletion	16355590	Y	N	N	Y	N	N

Intragenic region

para 3'UTR

A	B	C	D	E	F	G	H
C->T	16355625	Y	N	N	Y	N	N
C->A	16355656	Y	N	N	Y	N	N
C->T	16355682	Y	N	N	Y	N	N

During sequencing of the parental strains *w⁻ bss¹ f* and *w⁻ P[EP]EY00852*, 40 polymorphisms were detected in the chromosomal region between the *Rbp2* and *para* terminal exons. Column (A) shows the nature of each polymorphism, column (B) shows the molecular location on the chromosome. The presence or absence (Y or N) of each polymorphism in the parental strain is shown in columns (C) and (D), for convenience, the polymorphism pattern found in *w⁻ bss¹ f* chromosomes is shaded in grey while the polymorphism pattern for *w⁻ P[EP]EY00852* is unshaded. Columns (E-H) Four chromosomes that were the result of recombination events between *bss¹* and *P[EP]00852* (#1 - #4) were sequenced and their polymorphism patterns determined. The presence or absence (Y or N) of each polymorphism is shown. For convenience, where the pattern is that of the *w⁻ bss¹ f* parental strain it is shaded in grey, where the pattern is that of the *w⁻ P[EP]EY00852* parental strain it is unshaded. Recombination locations can be seen where the shading of the column changes from one parental strain to another. Column (E) shows that in chromosome #1, recombination took place between a TA→GG change at 16346958 and an A insertion at 16347422. Column (F) shows that in chromosome #2, recombination took place between an A→C change at 16350747 and an A→G change at 16351689. Column (G) shows that in chromosome #3, recombination also took place between A→C change at 16350747 and an A→G change at 16351689. These two chromosomes may be the complementary products of a single recombination event. Column (H) shows that in chromosome #4, recombination took place between a TTG deletion at 16353574 and an A→G change at 16354339. Recombinant chromosome #4 is the most informative as recombination took place within the *para* 3'UTR, meaning that the *bss¹* lesion must be to the right of this location, and therefore either within the *para* 3'UTR or one of the exons.